

Department of Cardiovascular Medicine, West China Hospital, Sichuan University, Chengdu, China

## Intermedin inhibits uptake of oxidized LDL via CD36 pathway in RAW264.7 cells

YONG WANG, RUI YANG, XIAONI CHEN, XIN ZHANG, SEN HE, JIAYUE FENG, SHIXI WAN, SI WANG, XIAOPING CHEN

Received November 21, 2013, accepted December 20, 2013

Xiaoping Chen, Department of Cardiovascular Medicine, West China Hospital, Sichuan University, Chengdu 610041, China  
chenxp0196@163.com

Pharmazie 69: 473–476 (2014)

doi: 10.1691/ph.2014.3941

Intermedin (IMD) exerts a potent function in preventing atherosclerosis, while the mechanism remains unclear. Here we investigated the potential molecular mechanism responsible for the protective function of IMD in preventing foam cell formation in RAW264.7 cells. In our present study, IMD significantly inhibited intracellular cholesterol accumulation. Additionally, IMD dose-dependently down-regulated CD36 expression, which was confirmed by real-time quantitative reverse transcription-PCR and Western blot analysis. Our data suggest that IMD could inhibit the formation of foam cells through, at least partly, a CD36-dependent mechanism. This study suggests that IMD may be a therapeutic candidate for treating atherosclerosis.

### 1. Introduction

According to common knowledge, the key events of atherosclerosis development are the uptake of oxidized low-density lipoprotein (ox-LDL) by macrophage and foam cell formation induced by intracellular cholesterol accumulation (Yu et al. 2013). Macrophages have been identified to express a number of scavenger receptors (Yu et al. 2013), among of which CD36 and class A scavenger receptor (SR-A) are reported to play important roles in uptake of ox-LDL.

Intermedin (IMD), also known as adrenomedullin-2, is a newly discovered peptide that belongs to the calcitonin gene-related peptide family (Roh et al. 2004; Takei et al. 2004). We have demonstrated that atherosclerotic plaque could be ameliorated by exogenous administration of IMD in ApoE<sup>-/-</sup> mice (Zhang et al. 2012). A recent study (Dai et al. 2012) has shown that IMD could inhibit SR-A in macrophages and thus decrease foam cell formation. We hypothesize that IMD could also inhibit CD36 in macrophages thereby counteracting atherosclerosis development. This present study prompts to explore the potential molecular mechanism of the anti-atherosclerosis function of IMD *in vitro*.

### 2. Investigations and results

#### 2.1. Cell viability

The cytotoxic effect of IMD on RAW264.7 cells was measured by CCK-8, and no cytotoxic effect was observed with up to 10<sup>-6</sup> mol/L of IMD (Fig. 1). Therefore, sample treatments between 10<sup>-8</sup> mol/L and 10<sup>-6</sup> mol/L were used in the subsequent experiments.

#### 2.2. IMD inhibits ox-LDL-induced cholesterol accumulation in RAW264.7 cells

Since cholesterol accumulation is the hallmark of foam cell formation, we explored whether IMD can inhibit this effect in

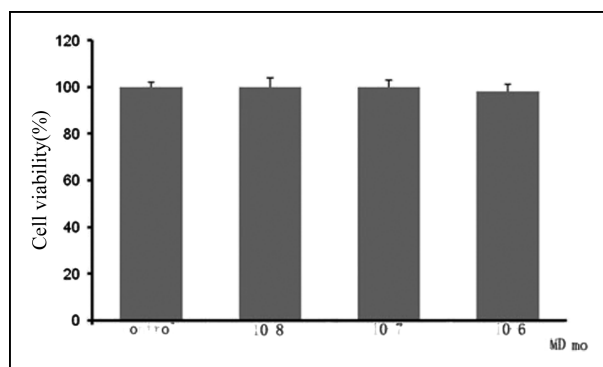


Fig. 1: Cell viability of RAW 264.7 macrophage cell line. RAW264.7 cells were treated with different concentrations of IMD (10<sup>-8</sup> mol/L, 10<sup>-7</sup> mol/L and 10<sup>-6</sup> mol/L) for 24 hours (n = 3). No cytotoxic effect was seen in each concentration.

murine RAW264.7 macrophage-like cells. As shown in Table 1, the intracellular cholesterol was examined by HPLC. The ox-LDL (50 mg/L) treated cells contain higher levels of total cholesterol than the control group. IMD treated cells show lower levels of intracellular cholesterol than the ox-LDL group without IMD, and this inhibitive effect indicates a dose-dependent manner. Consistently with HPLC data, the Oil red O staining also indicates the inhibitory effect of IMD on cholesterol accumulation in RAW264.7 cells (Fig. 2). The most lipid droplets were visualized in cells with ox-LDL, while the cells pretreated with IMD show less lipid droplets. The cells treated with the highest level of IMD (10<sup>-6</sup> mol/L) contained least lipid droplets.

#### 2.3. IMD regulates the expression of CD36

In view of the fact that CD36 is the major scavenger receptor for ox-LDL (Sun et al. 2007), we focused on testing the effects of IMD on it. As shown in Fig. 3, IMD can significantly attenuate the expression of mRNA CD36 in a dose-dependent manner,

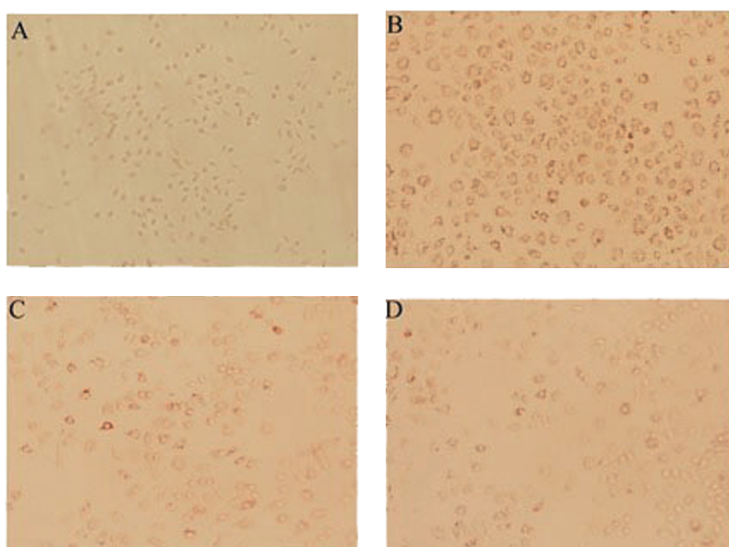


Fig. 2: Effects of IMD on formation of foam cell. Pretreated IMD can dose-dependently inhibit formation of foam cell, A. Control, B. ox-LDL 50 mg/ml, C. ox-LDL 50 mg/ml+ IMD  $10^{-7}$  mol/L, D. ox-LDL 50 mg/ml+ IMD  $10^{-6}$  mol/L.

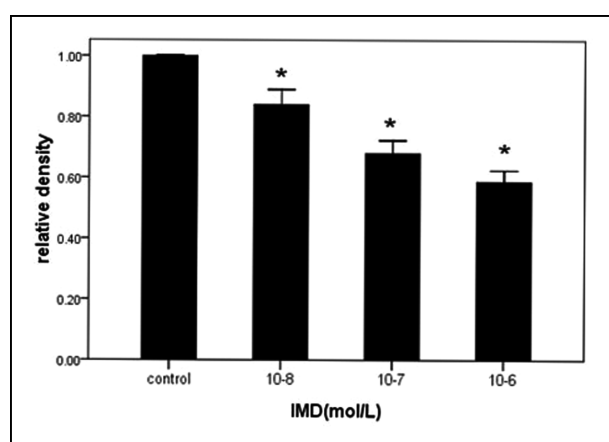


Fig. 3: Effects of IMD on mRNA level of CD36. IMD can dose-dependently down-regulate the transcription of CD36 ( $n=3$ ). Cells were treated with ox-LDL (as control) or ox-LDL plus various concentrations of IMD. \* $P < 0.05$ ; compared with control. Representative experiments are shown.

and the highest concentration ( $10^{-6}$  mol/L) of IMD can inhibit it by 41% (Fig. 3). In addition, the expression of CD36 protein level was also explored. Consistently with the trend of mRNA, the protein level of CD36 decreased with IMD concentrations (Fig. 4).

### 3. Discussion

Our previous study demonstrated that intravenous administration of IMD could ameliorate atherosclerotic plaque formation

**Table 1: Effect of IMD on intracellular cholesterol accumulation (mg/g protein)**

Group	Intracellular total cholesterol
Control	$166.4 \pm 10.3$
ox-LDL	$521.8 \pm 28.4^*$
ox-LDL + $10^{-8}$ mol/L IMD	$489.8 \pm 20.2$
ox-LDL + $10^{-7}$ mol/L IMD	$309.1 \pm 16.8\#$
ox-LDL + $10^{-6}$ mol/L IMD	$203.8 \pm 11.2\#$

Data are presented as mean  $\pm$  SD. \* $P < 0.05$  vs control. # $P < 0.05$  vs ox-LDL.

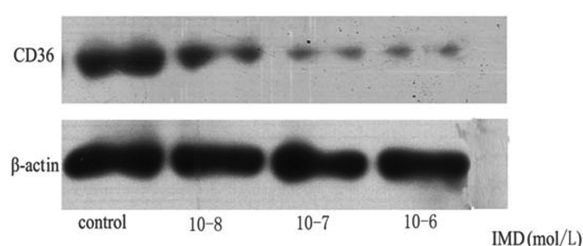


Fig. 4: Effects of IMD on protein expression level of CD36. IMD can dose-dependently down-regulate the expression of CD36. Cells were treated with ox-LDL (as control) or ox-LDL with various concentrations of IMD. A representative experiment is shown.

*in vivo*. Additionally, our present study showed that IMD administration can down-regulate CD36 expression at both the protein and mRNA level in RAW264.7 cells. Finally IMD attenuated ox-LDL uptake and accumulation in macrophages. Our results indicate the potent effects of IMD on reducing ox-LDL uptake and foam cell formation via CD36 pathway.

Macrophage uptake of oxidized low-density lipoprotein (ox-LDL) is generally believed to play a central role in foam cell formation and the pathogenesis of atherosclerosis (Nicholson et al. 2004). CD36 belongs to class B scavenger receptor which are the principal macrophage receptors responsible for the uptake of modified forms of LDL (Nicholson et al. 2004; Sun et al. 2007). Like SR-A, CD36 recognizes a broad variety of ligands including ox-LDL (Wang et al. 2011). SR-A and CD36 accounted for 75–90% of degradation of modified LDL while ox-LDL uptake was primarily mediated by CD36 (Yu et al. 2013). Previous studies showed that the blockade of CD36 exerted protective effect in atherosclerosis (Febbraio et al. 2000), and decreased expression of CD36 inhibited foam cell formation (Min et al. 2013). These findings suggest CD36 to be a potential target for preventing atherosclerosis. In this study we focused on investigating the regulatory effect of IMD on CD36 in the LDL metabolic pathway.

IMD, also known as adrenomedullin-2 (AM-2), is a newly discovered peptide that belongs to the calcitonin/calcitonin gene-related peptide family. Reports indicated that IMD peptide administration in rats induces blood pressure reduction, renal blood flow, and cardiac output (Fischer et al. 2002). Our previous study demonstrated that exogenous IMD could ameliorate vascular atherosclerotic lesions in an animal model (Zhang et al. 2012), with strong relationship to the human population

**Table 2: Primer sequences and product sizes for RT-PCR**

Primer	Sequence of primer	Product size (bp)
CD36 (for mice)		
Forward	5'-TGCAGGTCAACATATTGGTCAAGCC-3'	25
Reverse	5'-TGGTCCCAGTCTCATTAGCCACA-3'	24
$\beta$ -actin (for mice)		
Forward	5'-TGTGGATCGGTGGCTCCATCCT-3'	22
Reverse	5'-AACGCAGCTCAGTAACAGTCCG-3'	22

(Lv et al. 2013). Moreover, it can exert antioxidant action contributing to the antihypertrophic action (Liu et al. 2013). Dai et al. (2012) showed that IMD reduced intracellular total cholesterol levels and may inhibit LDL-induced transformation of macrophages to foam cells through down-regulation of gene expression and function of SR-A *in vitro*. In this present investigation, the expression of CD36 was markedly decreased by IMD administration in RAW264.7 cells, and this may be an alternative mechanism of IMD inhibiting foam cell formation. In addition to lipid uptake *via* scavenger receptors, many other aspects such as lipid transport, storage, metabolism, and efflux are involved in cellular lipid accumulation (Rigamonti et al. 2008). More studies are needed addressing the effects of IMD on gene expression which regulate multiple aspects of lipid homeostasis in cells.

In conclusion, IMD could ameliorate the formation of foam cell through, at least partly, a CD36-dependent mechanism, and this suggests that IMD may be a potential therapeutic candidate for treating atherosclerosis.

## 4. Experimental

### 4.1. Materials

RAW264.7 cells were purchased from Cell Bank in Shanghai Institutes for Biological Sciences, Chinese Academy of Sciences. Fetal bovine serum (FBS) and RPMI 1640 medium were obtained from HyClone (Logan, UT). Ox-LDL was purchased from the Peking Union Institute of Biochemistry (Beijing, China). Mouse IMD was purchased from Phoenix Pharmaceutical (Belmont, CA, USA) and Oil-Red-O was purchased from Sigma (St. Louis, MO, USA). Antibodies were from Santa Cruz Bio Inc. (Santa Cruz, CA). RT-PCR Kit was purchased from TaKaRa Bio Inc. (Dalian, China).

### 4.2. Cell culture and treatments

Cells were maintained in RPMI 1640 medium in 95% air and 5% CO<sub>2</sub> at 37 °C, supplemented with 2 mM L-glutamine, 100 U/ml penicillin and 100  $\mu$ g/ml streptomycin (Min 2013). When cells presented monolayer and confluence up to 70%, they were pretreated with various concentrations (10<sup>-8</sup> mol/L, 10<sup>-7</sup> mol/L and 10<sup>-6</sup> mol/L) of IMD (which was dissolved in DMSO) for 24 h, subsequently incubated with 50 mg/L of ox-LDL or 10% BSA for 24 h. Cells treated with equal amounts of DMSO were used as controls.

### 4.3. Cell viability

RAW264.7 cells were plated at a density of 1  $\times$  10<sup>4</sup> per well in a 96-well plate and incubated at 37 °C for 24 h. The cells were treated with different concentrations of IMD (10<sup>-8</sup> mol/L, 10<sup>-7</sup> mol/L and 10<sup>-6</sup> mol/L) for 24 h. After that cell counting kit-8 (CCK-8) reagent (Dojindo, Japan) was added for 4 h. Thereafter, the absorbance at 450 nm was measured using an enzyme-linked immunosorbent assay (ELISA) microplate reader (Benchmark; Bio-Rad Laboratories, CA, USA). Cell viability was calculated relative to that of the control group. All experiments were performed in triplicate.

### 4.4. High-performance liquid chromatogram analysis

The total cholesterol (TC) in cells was detected by high-performance liquid chromatogram (HPLC, Cullen et al. 1997). In brief, cells were scraped from the culture flasks and then washed 3 times with phosphate buffered saline (PBS), and then sonication was used to homogenize the cells for 10 s. After protein quantification with the BCA kit (Pierce Biotechnology,

Inc Rockford, USA), proteins included in the remaining supernatants were precipitated with an equal volume of cold KOH in ethanol (150 g/L), and vortexed until clear. After that an equal volume of 3:2 hexaneisopropanol (v/v) was added. The solution was vortexed and then centrifuged for 5 min (800 g, 15 °C). The organic phase was transferred to clean tapered glass tubes and dried under nitrogen at 40 °C, followed by adding 100  $\mu$ l isopropanol-acetonitrile (20:80, v/v). After solubilizing the sample in an ultrasound bath, centrifugation and transfer to the HPLC device cholesterol was eluted with 1 ml/min of eluent consisting of 20:80 isopropanol-acetonitrile (v/v) and detected by ultraviolet absorption at 206 nm. The total cholesterol was quantified by peak area.

### 4.5. Oil red O staining

Cells were washed three times with PBS and then fixed with 10% formalin at room temperature for 10 min. After being fixed, oil red O solution (60% saturated oil red O/40% deionized water) was used for staining at 37 °C for 30 min. For analysis, slides were then washed in isopropanol for 10 min, rinsed in tap water, counterstained with hematoxylin and mounted in glycerol/gelatin solution. And then images of cells were captured using an Olympus light microscope (Tokyo, Japan).

### 4.6. Quantitative RT-PCR analysis

Total RNA was extracted from cultured RAW264.7 cells using RNeasy Mini Kit (Qiagen, Crawley, UK) (Lam et al. 2006), followed by reverse transcription into cDNA using a SuperScript<sup>TM</sup> preamplification system (Invitrogen) according to the manufacturer's protocol. PCR was then performed to estimate the expression of CD36. The sequence-specific primers were presented in Table 2. After an initial denaturation for 5 min at 94 °C, sequential steps were performed as follows: denaturation at 94 °C for 1 min, annealing (60 °C for 1 min), extension (72 °C for 1 min) and a final extension of 72 °C for 10 min. The  $\beta$ -actin mRNA amplified from the same samples served as control.

### 4.7. Western blotting analysis

Whole cell lysates extracted from macrophages were washed with cold PBS and lysed in Tris-glycine buffer (0.25 M Tris, 0.173 M glycine) containing 3% SDS and 1 mM phenylmethylsulfonyl fluoride. The extracts were cleared in an Eppendorf centrifuge (20,000 g for 30 min at 4 °C). After separation by SDS-PAGE, proteins were transferred to a nylon/cellulose membrane. The membrane was blocked with PBS containing 0.1% Tween 20 and 3% fat-free milk for 2 h, followed by immunoblotting with antibodies for 10 h at 4 °C. The blots were incubated again with horseradish peroxidase-conjugated goat anti-rabbit IgG for 1 h at room temperature followed by three washes for 10 min each in washing buffer (TBS 1 0.05% Tween 20). Protein visualization on each immunoblot was developed and performed with DuPont Western blot chemiluminescence reagent. Rabbit polyclonal anti-CD36 was used at a concentration of 1:800.

### 4.8. Statistics

Data are reported as mean  $\pm$  SD. Student's t-test (two-tailed) was used to compare means between two groups.  $P < 0.05$  was taken as significant.

Acknowledgements: This study was supported by a project from the National Natural Science Foundation of China (Grant no: 30971269). No conflict of interest exists in the submission of this manuscript.

## References

Cullen P, Fobker M, Tegelkamp K, Meyer K, Kannenberg F, Cignarella A, Benninghoven A, Assmann G (1997) An improved method for quantification of cholesterol and cholesteryl esters in human monocyte-derived

- macrophages by high performance liquid chromatography with identification of unassigned cholesteryl ester species by means of secondary ion mass spectrometry. *J Lipid Res* 38: 401–409.
- Dai XY, Cai Y, Mao DD, Qi YF, Tang C, Xu Q, Zhu Y, Xu MJ, Wang X (2012) Increased stability of phosphatase and tensin homolog by intermedin leading to scavenger receptor A inhibition of macrophages reduces atherosclerosis in apolipoprotein E-deficient mice. *J Mol Cell Cardiol* 53: 509–520.
- Febbraio M, Podrez EA, Smith JD, Hajjar DP, Hazen SL, Hoff HF, Sharma K, Silverstein RL (2000) Targeted disruption of the class B scavenger receptor CD36 protects against atherosclerotic lesion development in mice. *J Clin Invest* 105: 1049–1056.
- Fischer JA, Muff R, Born W (2002) Functional relevance of G-protein-coupled-receptor-associated proteins, exemplified by receptor-activity-modifying proteins (RAMPs). *Biochem Soc Trans* 30: 455–460.
- Lam CW, Perretti M, Getting SJ (2006) Melanocortin receptor signaling in RAW264.7 macrophage cell line. *Peptides* 27: 404–12.
- Liu K, Deng X, Gong L, Chen X, Wang S, Chen H, Amrit B, He S (2013) The effect of intermedin on angiotensin II and endothelin-1 induced ventricular myocyte hypertrophy in neonatal rat. *Clin Lab* 59: 589–596.
- Lv Z, Wu K, Chen X, Zhang X, Hong B (2013) Plasma intermedin levels in patients with acute myocardial infarction. *Peptides* 43: 121–125.
- Min KJ, Um HJ, Cho KH, Kwon TK (2013) Curcumin inhibits oxLDL-induced CD36 expression and foam cell formation through the inhibition of p38 MAPK phosphorylation. *Food Chem Toxicol* 58: 77–85.
- Nicholson AC, Hajjar DP (2004) CD36 oxidized LDL and PPAR gamma: pathological interactions in macrophages and atherosclerosis. *Vascul Pharmacol* 41: 139–146.
- Rigamonti E, Chinetti-Gbaguidi G, Staels B (2008) Regulation of macrophage functions by PPAR-alpha, PPAR-gamma, and LXRs in mice and men. *Arterioscler Thromb Vasc Biol* 28: 1050–1059.
- Roh J, Chang CL, Bhalla A, Klein C, Hsu SY (2004) Intermedin is a calcitonin/calcitonin gene-related peptide family peptide acting through the calcitonin receptor-like receptor/receptor activity-modifying protein receptor complexes. *J Biol Chem* 279: 7264–7274.
- Sun B, Boyanovsky BB, Connelly MA, Shridas P, van der Westhuyzen DR, Webb NR (2007) Distinct mechanisms for OxLDL uptake and cellular trafficking by class B scavenger receptors CD36 and SR-BI. *J Lipid Res* 48: 2560–2570.
- Takei Y, Inoue K, Ogoshi M, Kawahara T, Bannai H, Miyano S (2004) Identification of novel adrenomedullin in mammals: a potent cardiovascular and renal regulator. *FEBS Lett* 556: 53–58.
- Wang N, Yin R, Liu Y, Mao G, Xi F (2011) Role of peroxisome proliferator-activated receptor- $\gamma$  in atherosclerosis: an update. *Circ J* 75: 528–535.
- Yu XH, Fu YC, Zhang DW, Yin K, Tang CK (2013) Foam cells in atherosclerosis. *Clin Chim Acta* 424: 245–252.
- Zhang X, Gu L, Chen X, Wang S, Deng X, Liu K, Lv Z, Yang R, He S, Peng Y, Huang D, Jiang W, Wu K (2012) Intermedin ameliorates atherosclerosis in ApoE null mice by modifying lipid profiles 37: 189–193.